Cellulose (2013) 20:597–603
DOI 10.1007/s10570-013-9866-x

ORIGINAL PAPER

$I_\alpha \rightarrow I_\beta$ transition of cellulose under ultrasonic radiation

Benjamin Briois · Tsuguyuki Saito · Christian Pétrier · Jean-Luc Putaux · Yoshiharu Nishiyama · Laurent Heux · Sonia Molina-Boisseau

Received: 10 July 2012 / Accepted: 15 January 2013 / Published online: 31 January 2013

Abstract Aqueous suspensions of dispersed *Glaucocystis* cellulose microfibrils were sonicated at 4 °C for 3 h, using 24 kHz ultrasonic waves. This treatment induced a variety of ultrastructural defects, as the microfibrils became not only shortened, but also presented substantial damage materialized by kinks and subfibrillation. Upon analysis by X-ray diffraction and ^{13}C solid-state NMR spectroscopy, it was found that the initial sample that contained 90 % of cellulose I_α allomorph became, to a large extent, unexpectedly converted into the I_β phase, while the loss of crystallinity was only moderate during the sonication treatment.

Keywords Cellulose microfibrils · Glaucocystis · Low frequency sonication · Allomorphic transition

B. Briois · J.-L. Putaux · Y. Nishiyama · L. Heux · S. Molina-Boisseau (✉)
Centre de Recherches sur les Macromolécules Végétales (CERMAV-CNRS), (affiliated with Université Joseph Fourier (UJF)), BP 53, 38041 Grenoble Cedex 9, France
e-mail: sonia.boisseau@cermav.cnrs.fr

T. Saito
Department of Biomaterials Sciences, Graduate School of Agricultural and Life Sciences, The University of Tokyo, Tokyo 113-8657, Japan

C. Pétrier
Laboratoire Rhéologie et Procédés, UMR 5520, BP 53, 38041 Grenoble Cedex 9, France

Introduction

Discovering that all native celluloses (cellulose I) were composed of two different allomorphs, namely cellulose I_α and I_β, has been one of the major landmarks leading to the comprehensive description of the crystalline ultrastructure of cellulose (Atalla and VanderHart 1984). As a result of this discovery, the various celluloses could be classified into two families. On the one hand, the celluloses from higher plants, such as wood, cotton, ramie, etc., were dominant in I_β; on the other hand, the celluloses from the cell wall of many green algae (*Valonia*, *Cladophora,* etc.), together with the cellulose produced by *Acetobacter xylinum*, were rich in the I_α allomorph (VanderHart and Atalla 1987; Horii et al. 1987a). At the extreme, tunicin, the cellulose from tunicates, which was found to be nearly 100 % I_β (Belton et al. 1989; Larsson et al. 1995) could be considered as a standard of the I_β phase, whereas the cellulose of the cell wall of the alga *Glaucocystis* could be selected as the nearly 100 % I_α standard counterpart (Sugiyama et al. 1991a; Imai et al. 1999).

The study of the crystal structure of both phases has revealed that the I_β phase was more compact with a crystal density of 1.63 as opposed to 1.61 for the I_α phase (Nishiyama et al. 2002, 2003). This difference in compactness is well in line with the thermodynamic stability of both phases. Indeed, it was shown that cellulose I_α could be converted into I_β in the solid state, following a severe hydrothermal treatment

(Horii et al. 1987b; Yamamoto et al. 1989; Yamamoto and Horii 1993; Debzi et al. 1991), whereas so far, the conversion of cellulose I_β into I_α has not been possible, despite a number of unpublished attempts. The difference of reactivity is another important feature that differentiates cellulose I_α from I_β. Indeed, in samples that contained a substantial proportion of both phases, a significant decrease in the amount of I_α phase was observed at the beginning of chemical (Sassi and Chanzy 1995) or enzymatic (Hayashi et al. 1998) reactions, a behavior that could be due, either to differences in intrinsic reactivity or to the topological distribution of the two phases. Thus, finding easy ways to interconvert cellulose I_α into I_β may have a great interest for modifying the reactivity of cellulose.

Besides the hydrothermal conversion of cellulose I_α into I_β, which is rather straightforward, but involves temperatures of 250 °C and above, two other more elaborate conversion routes have been described. They are based on the use of reversible solid-state transformations of cellulose fibers by (1) a fibrous acetylation, followed by saponification (Hirai et al. 1987) and (2) the conversion of cellulose I into cellulose III_I followed by a reversion into cellulose I (Chanzy et al. 1987).

In our search to find new ways to easily convert cellulose I_α into I_β, we have discovered that the use of ultrasonication was promising. This note describes how the conversion could be achieved by submitting cellulose microfibrils, rich in I_α phase, to low-frequency ultrasounds, in aqueous environment, at 4 °C.

Materials and methods

Cellulose

Glaucocystis nostochinearum, obtained from the IAM culture collection of the University of Tokyo was cultivated and its cellulose extracted and purified according to the methods described by Imai et al. (1999), leading to the preparation of *Glaucocystis* ghost cells in aqueous suspension. The ghost cells were dispersed into dimethylformamide (DMF) by solvent exchange. 2 % (w/w) of sulfamic acid with respect to DMF was then added and the suspension was heated and kept overnight at 80 °C under mild agitation, with the result of adding charged sulfate groups at the microfibril surfaces. The ghost cells were then washed by successive centrifugations into DMF, mixtures of isopropanol and DMF and finally into water where they spontaneously disrupted into non-flocculating suspensions of individual cellulose microfibrils.

Sonication

30 mL of a 0.1 wt% microfibril suspension was inserted into a specific reactor consisting of a cylindrical water-jacketed glass vessel. 24 kHz ultrasonic waves were emitted from the bottom of the vessel through the transducer surface area of an ultrasonic Hieschler high power sonoreactor UTR 200 operating at 50 W. The temperature of the ultrasonic bath was regulated at 4 °C by circulating cold water from an integrated cooling system. Sonication times up to 3 h were applied.

Transmission electron microscopy (TEM)

Drops of 0.001 % *Glaucocystis* microfibril suspension before and after sonication were deposited on glow-discharged carbon-coated TEM grids. The specimens were then negatively stained with 2 % uranyl acetate prior to complete drying and observed using a Philips CM200 'Cryo' microscope operating at 80 kV. Images were recorded on Kodak SO163 films.

X-ray diffraction (XRD)

Concentrated microfibril suspensions were allowed to dry onto flat Teflon surfaces. The resulting films were X-rayed with a Ni-filtered CuKα radiation ($\lambda = 0.15418$ nm), using a Philips PW3830 generator operated at 30 kV and 20 mA. The films were positioned perpendicular to the X-ray beam and diffraction patterns were recorded in transmission on Fujifilm imaging plates. XRD profiles were calculated by rotational averaging of the patterns.

Solid-state NMR spectroscopy

Samples were inserted into tightly sealed 4-mm BL-type ZrO_2 rotors. ^{13}C CP/MAS NMR spectra were recorded with a Bruker Avance spectrometer (100 MHz, ^{13}C) The spectra were acquired at room temperature with a 100 kHz proton dipolar decoupling

field, matched cross-polarization (CP) field of 80 kHz, a proton 90° pulse of 2.5 μs and magic angle spinning (MAS) at a spinning speed of 12 kHz. The cross-polarization transfer was achieved using a ramped amplitude sequence (RAMP-CP) for an optimized total time of 2 ms. A sweep width of 50,000 Hz was used to minimize baseline distortions. Fourier transform of the 2,944 points into 8k points was performed without apodization. The repetition time was 4 s and an average number of 20,000 scans was acquired for each spectrum. The ^{13}C chemical shifts were calibrated relative to the carbon chemical shift of the carbonyl signal of glycine at 176.03 ppm.

Results and discussion

A typical preparation of initial microfibrils from *Glaucocystis* cellulose is shown in Fig. 1a. As already described in the literature (Willison and Brown 1978; Imai et al. 1999) these microfibrils appear as slender and nearly endless straight filaments, each of them having a constant width and being devoid of any longitudinal defect. The microfibrils present a distribution in their diameter, with values ranging from 5 to 20 nm. In very few instances, tapered microfibril ends are also observed.

The effects of intensive sonication are shown in Fig. 1b–e. At a relatively low magnification (Fig. 1b), the images reveal that the microfibrils became not only shortened, but have also lost their initial rigidity due to a multiplication of kinks whose number increases with sonication time. When viewed at a higher magnification (Fig. 1c–e), the treated microfibrils present a succession of straight segments and kinks resulting in a peculiar "crankshaft" morphology in some regions or giving the impression of a smooth bending in others (Fig. 1c). At some kinks, the microfibrils are no longer compact, but are delaminated into a series of subfibrils having no more than 3 nm in width and maintaining

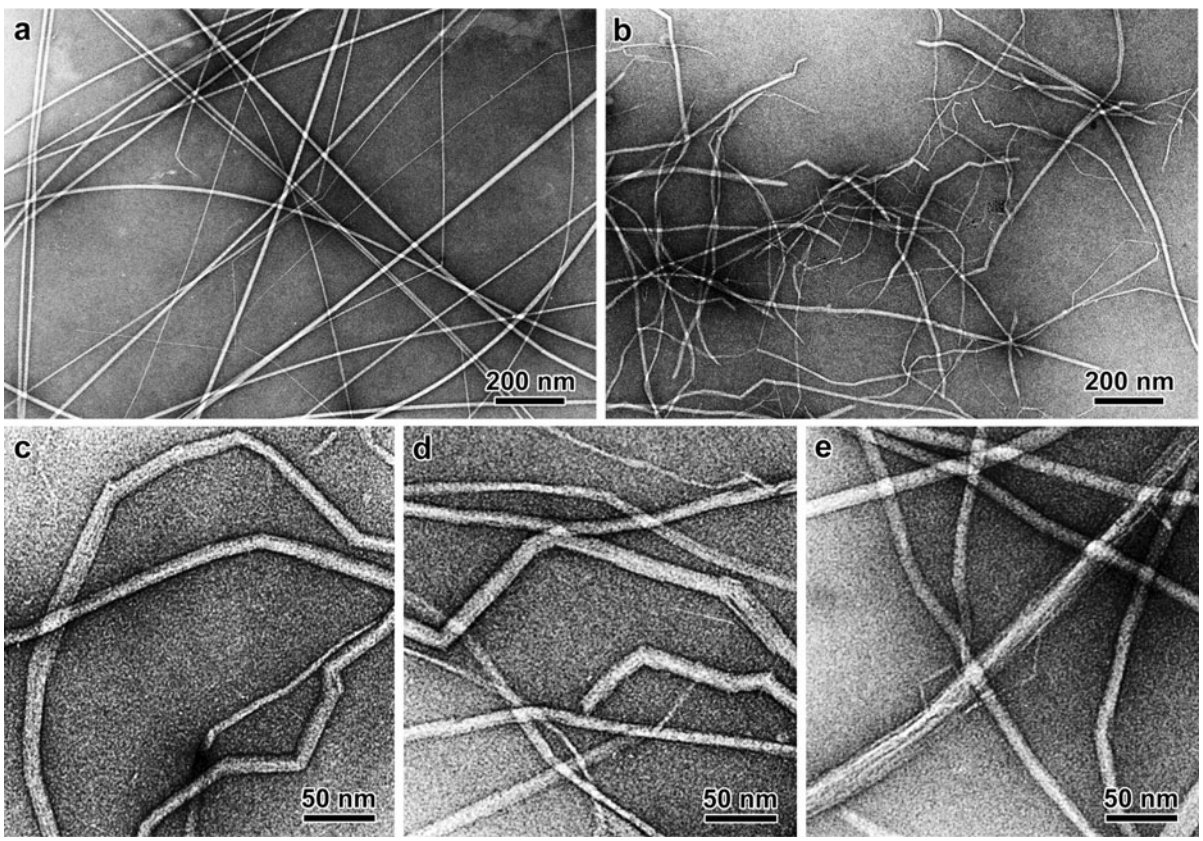

Fig. 1 TEM images of negatively stained *Glaucocystis* cellulose microfibrils before (**a**) and after (**b–e**) a 3 h sonication at 24 kHz. Images **c–e** are higher-magnification views of different types of defects observed after sonication

the continuity between the straight segments on each side of the kinks (well observed in Fig. 1d). Despite the significant damage resulting from the sonication, micron-long microfibrils are still observed and their longitudinal continuity is generally preserved (Fig. 1b). In a few microfibrils, a subfibrillation extending over several hundreds of nm is seen across a given segment. Some microfibrils are clearly delaminated into thinner subfibrils (Fig. 1e). As the number of very thin microfibrils increased in the observed preparations, it is likely that some subfibrils were completely individualized under mechanical homogenization.

The X-ray diffraction profiles of initial and sonicated cellulose microfibrils are shown in Fig. 2. As already reported (Imai et al. 1999; Nishiyama et al. 2003), the diffraction profile of the untreated microfibrils (Fig. 2a) corresponds to that of the cellulose I_α allomorph, with four main peaks, indexed in the triclinic unit cell as 100, 010, 002 and 110, located at 2θ diffraction angles of 14.4°, 16.8°, 20.2° and 22.6°, respectively. After sonication (Fig. 2b), the peaks at 14.4°, 20.2° and 22.6° have shifted toward higher angles with new 2θ values of ≈14.7°, 20.5°, 22.8°, respectively, whereas the peak at 16.8° did not shift. This new XRD profile and the position of the diffraction peaks bear many similarities with those recorded from a film of I_β-dominant tunicin nanocrystals (Fig. 2c), with diffraction peaks indexed as $1\bar{1}0$, 110, 102 and 200 in the I_β monoclinic unit cell, at diffraction angles of 14.7, 16.8, 20.5 and 22.8°, respectively (Nishiyama et al. 2002). The peak shifts between diffractograms 2a and 2b clearly indicate that a substantial transition from cellulose I_α to I_β has occurred during sonication. However, as the diffraction peaks are rather broad, the amount of each allomorph in the sample cannot be evaluated with precision. In the X-ray diffraction profile shown in Fig. 2b, the 010 peak is markedly reduced as opposed to the same peak in Fig. 2a. This feature indicates an uncommon uniplanar orientation of the cast film of the sonicated microfibrils.

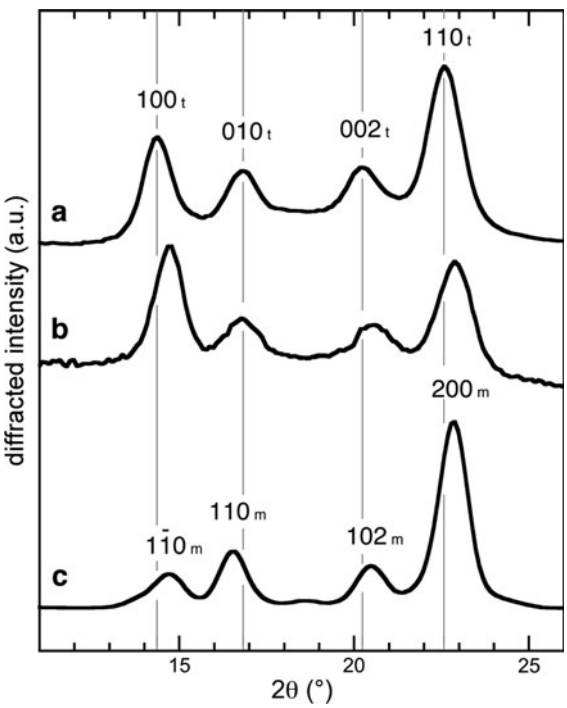

Fig. 2 X-ray diffraction profiles recorded from dry films of *Glaucocystis* cellulose microfibrils before (**a**) and after a 3 h sonication at 24 kHz (**b**). The profile recorded from a film of tunicate cellulose nanocrystals is shown for comparison (**c**). All films were oriented perpendicular to the incident X-ray beam. Subscripts t and m refer to the triclinic and monoclinic structure of allomorphs I_α and I_β, respectively. The indexing of the diffraction peaks was taken from unit cells defined by Sugiyama et al. (1991b)

Figure 3 shows the CP/MAS ^{13}C NMR spectra and their deconvolutions, of the initial (Fig. 3a) and sonicated microfibrils (Fig. 3b), together with those of *Valonia* cellulose (Fig. 3c) and tunicin (Fig. 3d), taken as references. In the initial sample, the C1 resonance appears nearly as a single sharp peak at 105.04 ppm, with two humps at the base of the peak. The C4 signal also occurs in the form of two main sharp resonances at 89.5 and 88.8 ppm and a small upfield hump, whereas the C6 signal appears as a sharp singlet at 65.1 ppm. These values and in particular those of the sharp peaks are typical of those attributed to I_α cellulose (Atalla and VanderHart 1984; VanderHart and Atalla 1984), in agreement with the spectrum of *Glaucocystis* which revealed that this cellulose contained close to 90 % of allomorph I_α (Imai et al. 1999).

New features are observed in the NMR spectrum of the cellulose sonicated during 3 h (Fig. 3b). The signal arising from the C1 carbon, which was nearly a singlet in the initial sample, is converted into a three-peak signal, with nearly equivalent resonances at 105.6, 105.14 and 104.1 ppm. The C4 signal is also substantially modified as it occurs as a rather broad resonance, with a central sharp peak centered at 88.8 ppm and two humps on both sides. The signal for

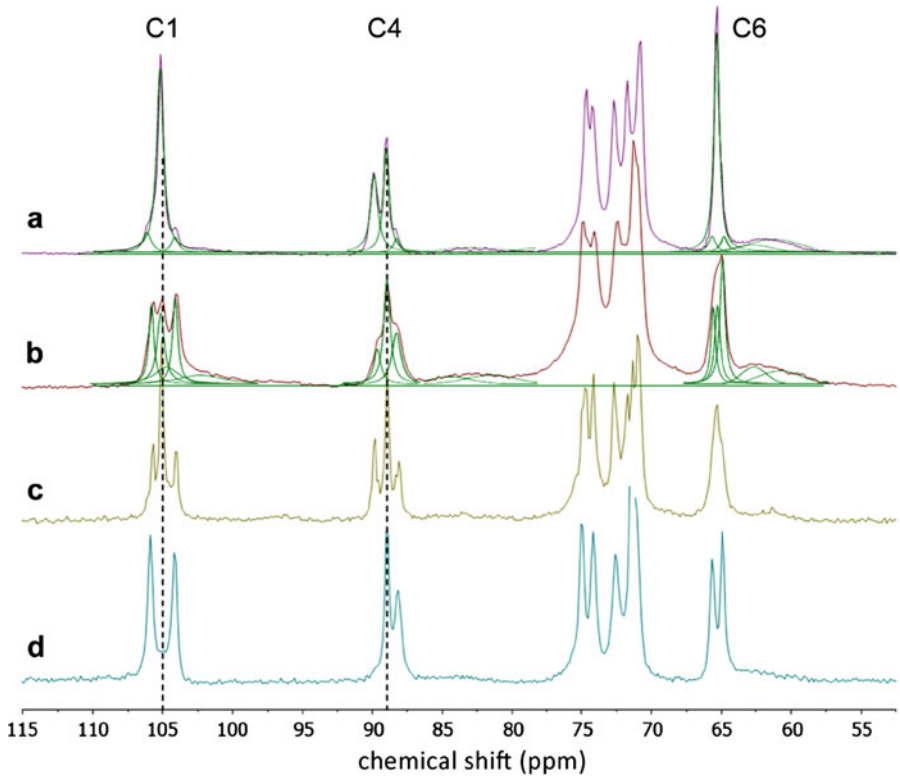

Fig. 3 CP/MAS ^{13}C NMR spectra of *Glaucocystis* cellulose before (**a**) and after a 3 h sonication at 24 kHz (**b**). Reference spectra of *Valonia* cellulose microfibrils (**c**) and tunicin nanocrystals (**d**) are presented for comparison

the C6 carbon still appears as an asymmetric signal with a maximum near 65.1 ppm, substantially broader than the corresponding resonance in the initial sample, thus indicating a composite substructure. The comparison of the spectra in Fig. 3 indicates that the spectrum of the sonicated *Glaucocystis* (Fig. 3b) can be deconvoluted into two subsets: one corresponding to that of the original sample and the other corresponding to that of tunicin, which is renown to be 90 % rich in cellulose I_β. This is particularly clear when considering the C1 resonance, where the two peaks at 105.6 and 104.1 ppm exactly correspond to those observed for the C1 signal of tunicin, whereas the central peak at 105.1 ppm corresponds to the sharp peak of the initial sample. The situation is less obvious for the C4 resonance, since despite the sharp protruding peak at 88.8 ppm, this resonance is rather broad in the sonicated sample. Nevertheless, the sharp resonance at 88.8 ppm is common to both I_α and I_β phases and each of the two humps can be assigned to one phase or the other 89.5 ppm for I_α and 88.2 for I_β. The shape of the resonance for the carbon C6 in Fig. 3b is consistent with the superposition of the singlet of the initial *Glaucocystis* at 65.1 ppm and the doublet of tunicin at 65.5 and 64.8 ppm.

The spectrum of the sonicated sample (Fig. 3b) can be compared with that of *Valonia* cellulose (Fig. 3c), which is known to be a 65:35 mixture of I_α and I_β (Wada et al. 2003; VanderHart and Atalla 1984; Yamamoto and Horii 1993; Heux et al. 1999). The overall shape appears as an envelope of the spectrum of the *Valonia* sample with apparently stronger contributions from the I_β sub-spectrum. In the present case, a deconvolution, using the treatment described elsewhere (Heux et al. 1999), confirms that after sonication, the amount of I_α phase in the *Glaucocystis* sample decreased from 90 to only 36 %, while, conversely, the I_β component increased from 10 % to 64 %. The position and width of the peaks used for the deconvolution are indicated in Table 1.

Another feature that can be deduced from the analysis of the spectra in Fig. 3 is the change of crystallinity after sonication. This variation is best deduced when considering the very broad resonance located upfield from the C4 sharp peaks, in the 80–86 ppm region. The comparison of this region in spectra 3a and 3b, after applying

Table 1 Chemical shift position and full width at half height (FWHH) of the peaks generated from the deconvolution of ^{13}C CP-MAS spectra of *Glaucocystis* cellulose before (a) and after (b) a 3 h sonication at 24 kHz

Peak	C1β	C1α	C1β'	C4β	C4α + β	C4α	C6β	C6α	C6β'
Position (ppm)									
(a)	105.6	105.0	103.9	89.5	88.8	88.2	65.5	65.1	64.8
(b)	105.7	104.9	103.8	89.6	88.7	88.1	65.3	65.1	64.7
FWHH (Hz)									
(a)	43	64	43	59	54	74	45	38	44
(b)	47	61	47	66	49	66	47	46	47

adequate deconvolution (Heux et al. 1999), indicates that the crystallinity of the samples, which was of the order of 72 % in the initial sample, is now reduced to 60 %.

The data presented here demonstrate that the use of a simple ultrasonic treatment is able to convert most of the crystalline I_α phase of *Glaucocystis* into I_β, while keeping intact most of the sample crystalline perfection. At the crystal level, the $I_\alpha \rightarrow I_\beta$ transition implies either a relative translation of one cellulose chain out of two by half a unit cell in the fiber direction, or the 180° rotation around the fiber axis of one chain out of two. In the present case, such movements may be the consequence of a transient intracrystalline swelling, taking its origin in the intense local heat liberated by the acoustic cavitation. Alternatively, chain movements could also be due to the shearing forces induced by the shockwaves resulting from the implosion of the cavitation bubbles, and to the deformations associated with the formation of kinks. The occurrence of the kinks and the subfibrillation observed in Fig. 1c–e are classical phenomena in the sonication of cellulose (Manley 1964; Frey-Wyssling et al. 1966). When the damaged microfibrils are submitted to successive cavitation events, the mechanical stress may be high enough to allow for some cracks to propagate along the microfibrils, resulting in the partial or complete separation of subfibrils.

In addition to the experimental conditions given here, there are many possibilities to vary the above experimental parameters, by modifying the geometry of the ultrasound reactor, the power and frequency of the ultrasound waves or the density of the sonication medium, etc. The effect of these variables on the I_α/I_β composition of the sonicated samples, their crystallinity and their ultrastructure are presently being investigated.

Conclusion

By submitting initially straight cellulose microfibrils from *Glaucocystis* to a 3 h low-frequency sonication, we have observed a variety of defects, in particular kinks and local or extended subfibrillation. This morphological change was accompanied by an unexpected allomorphic change from cellulose I_α to cellulose I_β. This remarkable effect of the ultrasonic treatment on both the ultrastructural and allomorphic features opens a way to new and interesting processes of cellulose modification at the nanometric scale.

Acknowledgments Funding for this project was provided by a grant from 'Région Rhône-Alpes'. The early contributions of M. Yunoki and Y. Doudaine to this work are acknowledged. We also thank M.-F. Marais for the culture of *Glaucocystis* and H. Chanzy for continuing support and critical reading of the manuscript.

References

Atalla RH, VanderHart DL (1984) Native cellulose: a composite of two distinct crystalline forms. Science 223:283–285

Belton PS, Tanner SF, Cartier N, Chanzy H (1989) High-resolution solid state ^{13}C nuclear magnetic resonance spectroscopy of tunicin, an animal cellulose. Macromolecules 22:1615–1617

Chanzy H, Henrissat B, Vincendon M, Tanner SF, Belton PS (1987) Solid-state ^{13}C-N.M.R. and electron microscopy study on the reversible cellulose I → cellulose III_I transformation in *Valonia*. Carbohydr Res 160:1–11

Debzi EM, Chanzy H, Sugiyama J, Tekely P, Excoffier G (1991) The $I_\alpha \rightarrow I_\beta$ transformation of highly crystalline cellulose by annealing in various mediums. Macromolecules 24:6816–6822

Frey-Wyssling A, Mühlethaler K, Muggli R (1966) Elementarfibrillen als Grundbausteine der nativen Cellulose. Holz Roh Werkst 24:443–444

Hayashi N, Sugiyama J, Okano T, Ishihara M (1998) Selective degradation of the cellulose I_α component in *Cladophora*

cellulose with *Trichoderma viride* cellulase. Carbohydr Res 305:109–116

Heux L, Dinand E, Vignon M (1999) Structural aspects in ultrathin cellulose microfibrils followed by ^{13}C CP-MAS NMR. Carbohydr Polym 40:115–124

Hirai A, Horii F, Kitamaru R (1987) Transformation of native cellulose crystals from cellulose I_b to I_a through solid-state chemical reactions. Macromolecules 20:1440–1442

Horii F, Hirai A, Kitamaru R (1987a) CP/MAS ^{13}C NMR spectra of the crystalline components of native celluloses. Macromolecules 20:2117–2120

Horii F, Yamamoto H, Kitamaru R, Tanahashi M, Higuchi T (1987b) Transformation of native cellulose crystals induced by saturated steam at high temperature. Macromolecules 20:2946–2949

Imai T, Sugiyama J, Itoh T, Horii F (1999) Almost pure I_α cellulose in the cell wall of *Glaucocystis*. J Struct Biol 127:248–257

Larsson PT, Westermark U, Iversen T (1995) Determination of the cellulose I_α allomorph content in a tunicate cellulose by CP/MAS 13C-NMR spectroscopy. Carbohydr Res 278: 339–343

Manley R, St J (1964) Fine structure of native cellulose microfibrils. Nature 204:1155–1157

Nishiyama Y, Langan P, Chanzy H (2002) Crystal structure and hydrogen-bonding system in cellulose I_β from synchrotron X-ray and neutron fiber diffraction. J Am Chem Soc 124:9074–9082

Nishiyama Y, Sugiyama J, Chanzy H, Langan P (2003) Crystal structure and hydrogen bonding system in cellulose I_α from synchrotron X-ray and neutron fiber diffraction. J Am Chem Soc 125:14300–14306

Sassi J-F, Chanzy H (1995) Ultrastructural aspects of the acetylation of cellulose. Cellulose 2:111–127

Sugiyama J, Persson J, Chanzy H (1991a) Combined infrared and electron diffraction study of the polymorphism of native cellulose. Macromolecules 24:2461–2466

Sugiyama J, Vuong R, Chanzy H (1991b) Electron diffraction study on the two crystalline phases occurring in native cellulose from an algal cell wall. Macromolecules 24: 4168–4175

VanderHart DL, Atalla RH (1984) Studies of microstructure in native celluloses using solid-state ^{13}C NMR. Macromolecules 17:1465–1472

VanderHart DL, Atalla RH (1987) Further carbon-13 NMR evidence for the coexistence of two crystalline forms in native celluloses. In: Atalla RH (ed.) The Structures of Cellulose. Characterization of the Solid States. ACS Symp Ser 340:88–118

Wada M, Kondo T, Okano T (2003) Thermally induced crystal transformation from cellulose I_α to I_β. Polym J 35:155–159

Willison JHM, Brown RM Jr (1978) A model for the pattern of deposition of microfibrils in the cell wall of *Glaucocystis*. Planta 141:51–58

Yamamoto H, Horii F (1993) CP/MAS ^{13}C NMR analysis of the crystal transformation induced for *Valonia* cellulose by annealing at high temperatures. Macromolecules 26:1313–1317

Yamamoto H, Horii F, Odani H (1989) Structural changes of native cellulose crystals induced by annealing in aqueous alkaline and acidic solutions at high temperatures. Macromolecules 22:4130–4132